

# Impact of power allocation strategies in long-haul few-mode fiber transmission systems

Danish Rafique,<sup>1,\*</sup> Stylianos Sygletos,<sup>2</sup> and Andrew D. Ellis<sup>2</sup>

<sup>1</sup>Nokia Siemens Networks, S.A. Lisbon, Portugal

<sup>2</sup>Aston Institute of Photonics Technologies, University of Aston, UK

\*[danish.rafique@nsn.com](mailto:danish.rafique@nsn.com)

**Abstract:** We report for the first time on the limitations in the operational power range of few-mode fiber based transmission systems, employing 28Gbaud quadrature phase shift keying transponders, over 1,600km. It is demonstrated that if an additional mode is used on a preexisting few-mode transmission link, and allowed to optimize its performance, it will have a significant impact on the pre-existing mode. In particular, we show that for low mode coupling strengths (weak coupling regime), the newly added variable power mode does not considerably impact the fixed power existing mode, with performance penalties less than 2dB (in Q-factor). On the other hand, as mode coupling strength is increased (strong coupling regime), the individual launch power optimization significantly degrades the system performance, with penalties up to ~6dB. Our results further suggest that mutual power optimization, of both fixed power and variable power modes, reduces power allocation related penalties to less than 3dB, for any given coupling strength, for both high and low differential mode delays.

©2013 Optical Society of America

**OCIS codes:** (060.1660) Coherent communications; (060.4256) Networks, network optimization; (060.4370) Nonlinear optics, fibers.

## References and links

1. R. Essiambre and A. Mecozzi, "Capacity limits in single mode fiber and scaling for spatial multiplexing," Optical Fiber Communication Conference, OFC '12, OW3D.1, (2012).
2. P. J. Winzer, "Energy-efficient optical transport capacity scaling through spatial multiplexing," IEEE Photon. Technol. Lett. **23**(13), 851–853 (2011).
3. E. Ip, N. Bai, Y. Huang, E. Mateo, F. Yaman, S. Bickham, H. Tam, C. Lu, M. Li, S. Ten, A. P. T. Lau, V. Tse, G. Peng, C. Montero, X. Prieto, and G. Li, "88x3x112-Gb/s WDM transmission over 50-km of three-Mode fiber with inline multimode fiber amplifier," European Conference on Optical Communication, ECOC'11, Th.13.C.2, (2011).
4. T. Hayashi, T. Sasaki, and E. Sasaoka, "Multi-core fibers for high capacity transmission," Optical Fiber Communication Conference, OFC '12, OTu1D.4, (2012).
5. S. Randel, R. Ryf, A. Gnauck, M. A. Mestre, C. Schmidt, R. Essiambre, P. Winzer, R. Delbue, P. Pupalaiakis, A. Sureka, Y. Sun, X. Jiang, and R. Lingle, "Mode-multiplexed 6x20-GBd QPSK transmission over 1200-km DGD-compensated few-mode fiber," Optical Fiber Communication Conference, OFC '12, PDP5C.5, (2012).
6. A. Mecozzi, C. Antonelli, and M. Shtaif, "Nonlinear propagation in multi-mode fibers in the strong coupling regime," Opt. Express **20**(11), 11673–11678 (2012).
7. C. Koebele, M. Salsi, G. Charlet, and S. Bigo, "Nonlinear effects in mode-division-multiplexed transmission over few-mode optical fiber," IEEE Photon. Technol. Lett. **23**(18), 1316–1318 (2011).
8. N. MacSuihbhne, R. Watts, S. Sygletos, F. C. G. Gunning, L. GrüNernielsen, and A. D. Ellis, "Nonlinear pulse distortion in few-mode fiber," European Conference on Optical Communication, ECOC'12, Th.2.F.5, (2012).
9. J. M. Kahn, K. Ho, and M. B. Shemirani, "Mode coupling effects in multi-mode fibers," Optical Fiber Communication Conference, OFC '12, OW3D.3, (2012).
10. J. Vuong, P. Ramantanis, A. Seck, D. Bendimerad, and Y. Frignac, "Understanding discrete linear mode coupling in few-mode fiber transmission systems," European Conference on Optical Communication, ECOC'11, Tu5B2, (2011).
11. P. Sillard, M. Bigot-Astruc, D. Boivin, H. Maerten, and L. Provost, "Few-mode fiber for uncoupled mode-division multiplexing transmissions," European Conference on Optical Communication, ECOC'11, Tu5C7, (2011).
12. G. Rademacher, S. Warm, and K. Petermann, "Analytical description of cross-modal nonlinear interaction in mode multiplexed multimode fibers," IEEE Photon. Technol. Lett. **24**(21), 1929–1932 (2012).
13. D. Marcuse, *Theory of Dielectric Optical Waveguides*, chapters 3&5, (Academic, 1974).

14. F. Ferreira, S. Jansen, P. Monteiro, and H. Silva, "Nonlinear semi-analytical model for simulation of few-mode fiber transmission," *IEEE Photon. Technol. Lett.* **24**(4), 240–242 (2012).
15. G. Agrawal, *Applications of nonlinear Fibre Optics* chapter 2, (Academic Press, 2001).
16. F. Gardner, "A BPSK/QPSK timing-error detector for sampled receivers," *IEEE Commun. Mag.* **34**, 423–429 (1986).
17. S. Savory, "Digital signal processing for coherent systems," *Optical Fiber Communication Conference, OFC '12, OTh3C.7*, (2012).
18. D. V. Borne, C. R. S. Fludger, T. Duthel, T. Wuth, E. D. Schmidt, C. Schullien, E. Gottwald, G. D. Khoe, and H. de Waardt, "Carrier phase estimation for coherent equalization of 43-Gb/s POLMUXNRZ-DQPSK transmission with 10.7-Gb/s NRZ neighbours," *European Conference on Optical Communication, ECOC'107, 7.2.3*, (2007).
19. S. Mumtaz, R. Essiambre, and G. P. Agrawal, "Reduction of nonlinear penalties due to linear coupling in multicore optical fibers," *IEEE Photon. Technol. Lett.* **24**(18), 1574–1576 (2012).
20. X. Chen, J. E. Hurley, M.-J. Li, and R. S. Vodhanel, "Effects of multipath interference (MPI) on the performance of transmission systems using Fabry-Perot lasers and short bend insensitive jumper fibers," *Optical Fiber Communication Conference, OFC '09, NWC5*, (2009).

---

## 1. Introduction

With the ever increasing demand for high information rates and current advances in bandwidth intense user-end applications (online gaming, ubiquitous video, etc.), the available transmission capacity for single mode optical fiber is exhausting at a very fast rate, and radical solutions are now sought in order to be able to keep up with rapidly growing traffic demand. One of the solutions to enable significant capacity scale-up is space division multiplexing, or spatial multiplexing [1–3]. Spatial multiplexing increases transmission capacity by multiplexing several data signals in the cores of multicore fibers (MCFs) [4] or in the modes of multimode fibers (MMFs), in which case, it is often called mode-division multiplexing (MDM) [5].

While MDM solutions enable high capacity growth, these systems present complex trade-offs to system designers. One such challenge is associated with linear and nonlinear mode coupling effects, which strongly connect the achieved capacity to the achievable transmission distance [6–8]. Index perturbations in fibers, whether intended or not, can induce coupling between signals in different modes, and can cause propagating fields to evolve randomly. Mode coupling can significantly impact the transmission performance in several ways, i.e. crosstalk between spatially multiplexed signals, end-to-end group delay spread of signals, mode dependent loss/gain, etc [9]. Recently, a few preliminary reports analyzing propagation impairments considering both linear [10] and nonlinear coupling [6] have been reported, however the recent developments in spatially multiplexed systems demand not only a deeper and clearer understanding of coupling effects, but also their impact on system design choices.

One of the system design parameters is related to launch power optimization of individual modes in a multi-mode fiber based transmission system. Given that mode conversion, coupling, etc. are considered an essential part of a mode division multiplexed system, leading to modal crosstalk, it is critical to analyze the impact of individual optimal mode launch powers, since various modes have different propagation characteristics.

In this paper we consider the optimum signal launch power strategies, described in Table 1, in a bi-modal spatially multiplexed few-mode fiber transmission system, employing 28Gbaud coherent quadrature phase shift keying (QPSK) modulation, with a total transmission distance of 1,600km. We consider two case studies corresponding to high and low differential mode delay as a function of the linear mode coupling strength. We observe that in the absence of linear mode coupling the relative powers in the two modes has negligible impact on transmission performance in both cases, due to insignificant inter modal crosstalk –dependent on the fiber type. However as the mode coupling strength is increased significant performance penalties of up to ~6dB are observed for strongly coupled transmission regimes. We further show that in this case such penalties may be minimized by an appropriate balance of launch powers, and identify the relative impact of linear and nonlinear mode coupling on the optimum power levels.

Table 1. Power allocation strategies for bi-modal transmission system

	Homogenous power optimization	Mutual power optimization	Individual power optimization
Power of first mode	Variable	Fixed/Variable	Fixed/Variable
Power of the second mode	Variable	Variable/Fixed	Variable/Fixed
Performance metric	Mean Q-factor	Mean Q-factor	Q-factor of variable power mode

## 2. Simulation model

Figure 1 shows the simulation setup, where we investigate transmission of pairs of modes. In order to focus on the power allocation strategies, we consider propagation in a fictitious two-mode fiber, and consider two cases with a large difference in propagation constant. Detailed parameters for these fictitious fibers were inspired by fibers described in [11], corresponding to  $LP_{01,21}$  (high differential mode delay (DMD), 4007ps/km) and  $LP_{21,02}$  (low DMD, 426ps/km). The two values of DMD correspond to regimes where previous works [8] have observed weak nonlinear mode coupling (high DMD) due to walk off and strong nonlinear mode coupling (low DMD). Note that the low DMD case has a sufficiently high difference in phase velocity to ensure that FWM effects [12] remain negligible for both fibers. The formulation of our model is based on the initial work of Marcuse [13] that assumes periodic variation of the core's radius along the longitudinal axis of a multimode fiber, representing worst-case transmission scenario with respect to mode coupling as used by several authors recently [7, 14]. Note that for simplicity the spatial degeneracy of the  $LP_{21}$  mode is ignored in our model and that the two key parameters are influenced by the overall fiber design (DMD) and the fabrication conditions (coupling strength).

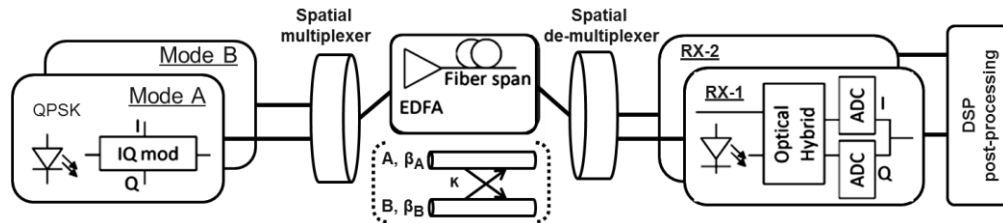


Fig. 1. Simulation setup for few-mode fiber transmission over 1,600km, employing 28Gbaud QPSK modulation, and digital signal processing at the receiver. I: Inphase, Q: Quadrature,  $\kappa$ : Coupling efficiency, EDFA: Erbium doped fiber amplifier, ADC: Analog-to-digital-converter.

The transmission system comprised of two 28Gbaud QPSK transponders, for each of the two emulated bi-modal fibers. For each fiber, independent de-correlated De Bruijn bit sequences (DBBS) of length  $2^{14}$ , with different random number seeds were used. Each DBBS was coded into two two-level output symbol stream, optically modulated as an in-phase and a quadrature phase carrier using a continuous wave laser source (1550nm) and a nested Mach-Zehnder Modulator structure. After modulation the two modes were combined using an ideal mode multiplexer (inter mode crosstalk at the transmitter was neglected). The simulation conditions ensured 16 samples per symbol with  $2^{13}$  (8192) total simulated symbols per mode, corresponding to a total 32,768 bits (one detected error corresponding to a bit error rate of  $3 \times 10^{-5}$ ). As an initial condition the modes had the same average power level. For simplicity we also neglected polarization mode dispersion and laser line-width in this paper.

The mode division multiplexed signal was propagated over a few-mode fiber. The linear mode coupling effects in a few-mode fiber are well described by traditional coupled mode theory [13, 15], applied on a simplified model of the optical fiber that assumes step index waveguide geometry with a sinusoidal deformation of the radius at the core-cladding interface. Following the corresponding derivation process in [15] and accounting for

nonlinearity through the introduction of inter and intra mode effective areas, it is found that the slowly varying field envelopes  $A_m(z, t)$ , with  $m = 1, 2$  of two co-polarized optical modes, defined with respect to a common rapidly varying part of  $\exp[i(\omega t - \beta z)]$ , are governed in the time domain by the following set of coupled propagation equations:

$$\frac{\partial A_1}{\partial z} - i\delta_a A_1 + \frac{1}{v_{g1}} \frac{\partial A_1}{\partial t} - i \frac{\beta_{21}}{2} \frac{\partial^2 A_1}{\partial t^2} + \frac{\alpha}{2} = -i\kappa A_2 - i \frac{n_2 \omega}{c} (f_{11} |A_1|^2 + 2f_{12} |A_2|^2) A_1 \quad (1)$$

$$\frac{\partial A_2}{\partial z} + i\delta_a A_2 + \frac{1}{v_{g2}} \frac{\partial A_2}{\partial t} - i \frac{\beta_{22}}{2} \frac{\partial^2 A_2}{\partial t^2} + \frac{\alpha}{2} = -i\kappa A_1 - i \frac{n_2 \omega}{c} (f_{22} |A_2|^2 + 2f_{21} |A_1|^2) A_2 \quad (2)$$

where the parameters of  $\beta = (\beta_{01} + \beta_{02})/2$  and  $\delta_a = (\beta_{01} - \beta_{02})/2$  have been introduced with  $\beta_{0m}$  representing the propagation constant of the  $m^{\text{th}}$  mode. Also,  $v_{gm} = 1/\beta_{1m}$  represents the group velocity,  $\beta_{2m}$  the group-velocity dispersion (GVD),  $\alpha$  is the loss coefficient,  $n_2$  the nonlinear refractive index and  $c$  the speed of light. The linear and nonlinear coupling mechanisms appear on the right-hand side of the above equations. The coupling coefficient  $\kappa$  introduces a periodic exchange of optical power between the two co-propagating modes. The maximum ratio of optical power that is transferred from the one to the other mode is defined by the coupling strength factor  $F = \kappa^2 / (\kappa^2 + \delta_a^2)$ , and occurs within a coupling length of  $L_c = \pi / 2\sqrt{\kappa^2 + \delta_a^2}$ . On the other hand, the nonlinear interactions due to Kerr effect can occur either within the same mode or between different modes, and their relative magnitude is governed by the overlapping integral  $f_{pq}$ :

$$f_{pq} = \frac{\iint |F_p(x, y)|^2 |F_q(x, y)|^2 dx dy}{\iint |F_p(x, y)|^2 dx dy \iint |F_q(x, y)|^2 dx dy} \quad (3)$$

where  $p, q = \{1, 2\}$  and with  $F_p(x, y)$  and  $F_q(x, y)$  representing the spatial distribution of the corresponding modes. Some details on the model can be found in [15]. Also, it is worth mentioning that more advanced modeling approaches have been elaborated as well, e.g [6], assuming isotropic mode coupling statistics, and thus generalizing the Manakov theory for multimode fibres; however in the next sections we will clearly demonstrate that in the regimes of interest, the qualitative conclusions are well predicted by our model. The total transmission distance was fixed to 1,600km, and the link consisted of 80km spans, no inline dispersion compensation and single-stage erbium doped fiber amplifiers (EDFAs). We considered equal loss coefficients for all the modes, and additional mode coupling at splices and amplifier sites was neglected to focus on the power allocation related nonlinear dynamics. Note that the upper bound on the step-size was set to be 1 km and the step length was chosen adaptively during the integration along the fiber based on the condition that in each step the nonlinear effects must change the phase of the optical field by no more than 0.05 degrees. Note that we independently verified the dependence of performance on step length (as low as 1m) for the scenarios considered in work, and found the results to be largely independent of the step-size. In this study a fiber of step index profile has been considered, with a core radius of 10.6 $\mu\text{m}$  and a numerical aperture of 0.12, corresponding to a normalized frequency [13, 15] of 5.1@ $\lambda$ :1550nm. The rest of the fiber parameters are given in Table 2. Each amplifier stage was modeled with a 4.5 dB noise figure and the total amplification gain was set to be equal to the total loss in each span. At the coherent receiver the received signal was ideally mode demultiplexed, filtered with a 56 GHz 3rd order Gaussian filter, coherently-detected (one for each mode) using balanced detectors to give the baseband electrical signal and sampled at 2 samples per symbol. Digital signal processing consisted of conventional steps, including clock

recovery using Gardner algorithm [16], frequency domain equalization of chromatic dispersion for each mode, followed by multiple input multiple output (MIMO) equalization of the two modes in a 2x2 structure employing finite impulse response (FIR) filters (T/2-spaced taps) adapted using blind constant modulus algorithm (CMA) [17]. Finally phase estimation was performed using Viterbi and Viterbi algorithm (this was done to minimize the impact of high frequency nonlinear effects [18] and rotate the constellation in the correct direction), followed by symbol decisions and performance assessment using Q-factors. All the numerical simulations were carried out using MATLAB® v7.11.

**Table 2. Fiber parameters at 1550nm (D: dispersion,  $A_{\text{eff}}$ : effective area,  $\alpha$ : loss,  $n_2$ : nonlinear index, V: normalized frequency)**

Parameters	$LP_{01}$	$LP_{21}$	$LP_{02}$
D (ps/nm/km)	15.19	13.86	9.48
$A_{\text{eff}}$ ( $\mu\text{m}^2$ )	248	229	255
$A_{\text{eff}01,21}$ ( $\mu\text{m}^2$ )		556	
$A_{\text{eff}21,02}$ ( $\mu\text{m}^2$ )		704	
$\alpha$ (dB/km)		0.2	
$n_2$ ( $\text{m}^2/\text{W}$ )		$2.6 \times 10^{-20}$	
V		5.1	

### 3. Results and discussions

In order to gain insight on the dependence of optimal launch power allocation on nonlinear inter modal crosstalk (or nonlinear coupling) in Fig. 2 we set the linear mode coupling to be zero. The modes are termed as fast and slow modes ( $LP_{01}$  and  $LP_{21}$ , in the high DMD fiber and  $LP_{02}$  and  $LP_{21}$  in the low DMD fiber, respectively).

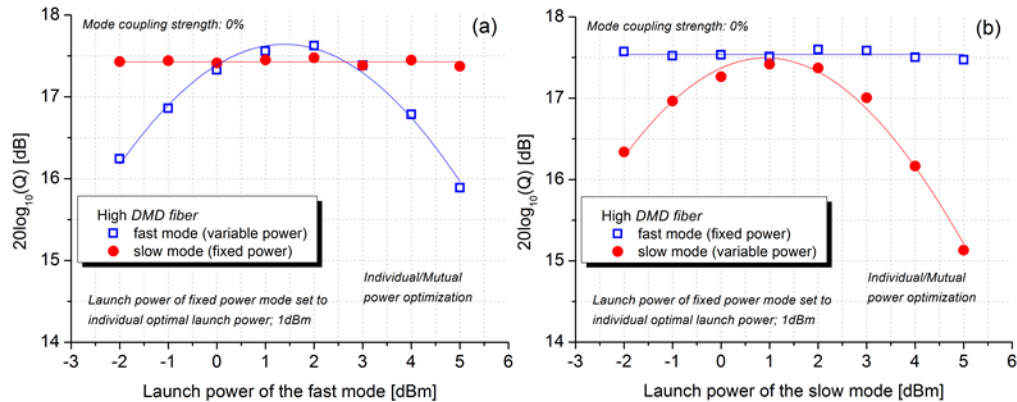


Fig. 2. Q-factor [dB] as a function of launch power [dBm], for QPSK transmission over 1,600km of the high DMD fiber with zero mode coupling. a) Launch power of the fast mode (open squares) is varied and launch power of the slow mode (solid circles) is fixed. b) Launch power of the slow mode is varied and launch power of the fast mode is fixed (symbols unchanged). (This figure represents a case of individual/mutual power optimization)

Figure 2 illustrates the performance in Q-factor after a total transmission distance of 1,600km for high DMD fiber, where the power of one mode was first optimized in single mode transmission (approximately 1dBm in both cases), and then the power of the second mode was swept (a case of both individual and mutual power optimization). It can be seen that as the launch power of the second mode is varied, the transmission performance is initially limited by optical signal-to-noise ratio (OSNR), and reaches an optimum power (also known as nonlinear threshold – NLT), beyond which performance is degraded due to nonlinear fiber impairments. Two key conclusions can be drawn from Figs. 2, 1) as the launch power of second channel is varied; the performance of first channel is virtually unaffected. 2) The optimal performance of the second channel is similar to that of the first channel, even

after –worst case (see Table 1)- individual launch power optimization (i.e. mutual power optimization does not play any role). Both of these conclusions can be attributed to the absence of linear mode coupling. Note that the penalties may increase in a WDM system, where strongly phase matched spectral regions will exist [12].

As we would expect, given the low difference in the effective area of the modes, the relative launch power in the two modes has negligible impact in the absence of linear mode coupling. In the rest of the paper we systematically investigate the impact of linear mode coupling strength on the transmission performance for various power allocation strategies, both for high DMD and low DMD fibers. Figure 3(a) plots the Q-factor as a function of launch power per mode, for MDM few-mode transmission, for the case of equal launch powers for the two modes (homogenous optimization) at a mode coupling strength of 5%. It can be seen that with finite linear mode coupling, the transmission performance for low DMD fiber is worse than that of high DMD mode pair fiber. This performance is consistent with the fundamental behavior of increased mode coupling efficiency with reduced DMD, essentially worsening the transmission performance (more details to follow). Figure 3(b) and Fig. 3(c) qualitatively show the performance for high and low DMD transmission, for the fast and slow modes, respectively, consistent with uncorrelated noise sources and a high Q factor. Note that, with 5% linear mode coupling, the transmission performance is degraded by ~3dB for the high DMD fiber and 4dB for the low DMD fiber, compared to the case with no linear coupling (as shown in Fig. 2). This behavior can be attributed to increase in crosstalk with increasing mode coupling strength.

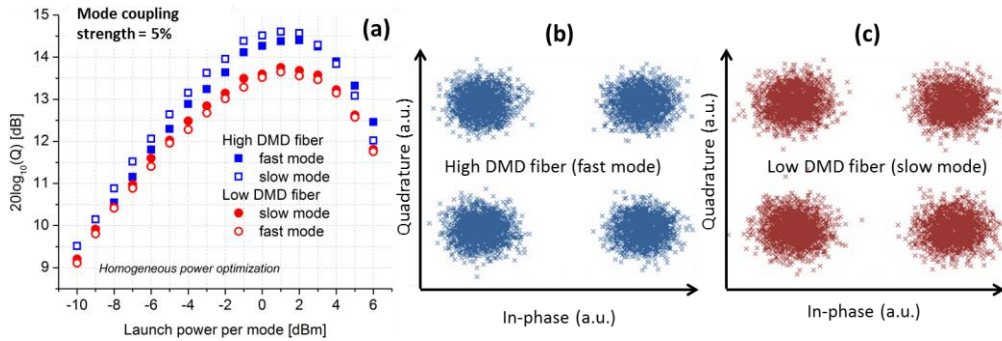


Fig. 3. a) Q-factor [dB] as a function of launch power per mode [dBm], for QPSK transmission over 1,600km with 5% mode coupling strength, for high DMD fiber (blue squares) showing slow (open) and fast (solid) modes and low DMD fiber (red circles) for slow (solid) and fast (open) modes. b&c) Constellation plots, at optimum launch power of 1dBm, for b) fast mode transmitted over high DMD fiber, and c) slow mode transmitted over low DMD fiber. (This figure represents a case of homogenous power optimization).

The impact of linear mode coupling strength on the transmission performance is shown in Fig. 4, where we plot the system performance as a function of mode coupling strength employing homogeneous power optimization (equal powers in both modes), and each point taken at the optimal power from a plot similar to Fig. 3(a). As seen in Fig. 4(a), with increasing mode coupling strength, the transmission performance monotonically decreases for both fibers. Moreover, it can be seen that the degradation of the high DMD fiber is slower than for the low DMD fiber as expected from the increased impact of linear mode coupling with lower DMD. However, whilst the overall behavior is consistent with our understanding of linear mode coupling effects, in Fig. 4(b) we plot the contribution of nonlinearity to the Q-factor penalty as a function of mode coupling strength. The penalty is calculated by subtracting the results of Fig. 4(a) from purely linear transmission at similar optimal launch power per mode. The value of ~1.4dB at 0% mode coupling strength corresponds to the typical nonlinearity penalty observed at the optimum launch power for conventional single mode transmission systems. As the mode coupling strength is increased, the net nonlinear penalty reduces, more rapidly for the low DMD fiber, confirming that mode coupling reduces



the impact of nonlinearity as recently observed in [19], although the reduction in nonlinear penalty suggests that the reduction is due to a complex interaction of effects including cross mode nonlinearity, linear mode coupling and DSP convergence.. The net effect is thus dominated by linear mode coupling, and whilst this may, in principle, be compensated with an ideal receiver, it is un-compensable using practical blind DSP [10] as used in this paper.

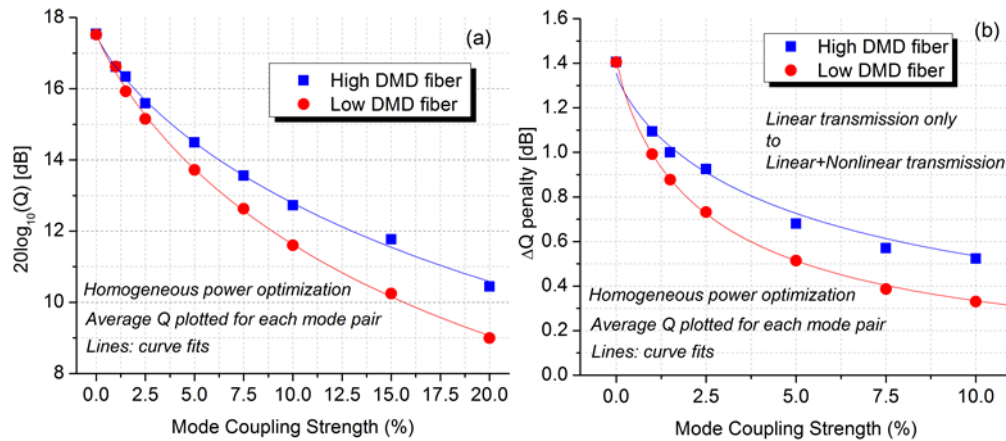


Fig. 4. a) Q-factor as a function of mode coupling strength [%], for QPSK transmission over 1,600km, for high (square) and low (circle) DMD fiber. b) Nonlinear Q-factor penalty difference (Q factor at optimum launch power and Q factor without nonlinearity at the same launch power) as a function of mode coupling strength [%], for high (square) and low (circle) DMD fiber. (This figure represents a case of homogenous power optimization).

Having established that linear crosstalk dominates the performance for homogenous power allocation (equal power in each mode), in Fig. 5, we report the impact of individual and mutual launch power strategies, and show the performance, in Q-factor, of both modes, as a function of launch power of one of them, after a total transmission distance of 1,600km using both fiber types. Note that the launch power of one is fixed at the previously established optimal launch power of 1dBm. It can be seen that as the launch power of either of the modes is increased towards its optimal value, the transmission performance of the fixed power mode degrades significantly. This behavior can be attributed to increased coherent crosstalk arising from a higher power being linearly coupled to the fixed mode when the launch power is increased [20]. Note that, contrary to homogenous power optimization, the optimum launch power of the mode with variable power is different to its value in isolation (1dBm). This may be explained by considering the intra mode nonlinear penalty and the inter mode linear crosstalk penalty simultaneously. At this level of mode coupling, the linear crosstalk penalty is around 3dB, with an additional 1dB from intra mode nonlinearity. However, to first order if the signal power is increased the ratio of the signal power within the channel to the linear crosstalk arising from the fixed power channel reduces, reducing the linear crosstalk penalty more rapidly than the nonlinear penalty increases. Eventually the nonlinear penalty begins to dominate the performance, and the new optimum launch power is achieved, At this new optimum power level, as shown in Fig. 5, the performance of fixed power mode is reduced by a further ~3dB and ~4dB for high and low DMD fibers, respectively whilst the optimum performance of the variable power channel is only increased by 1dB at most, where almost identical performance is observed irrespective of the effective area of the mode carrying the variable power channel.

The aforementioned penalties in transmission performance, given the potential to vary the power in each mode, give rise to a critical question as to how the launch power should be optimized. In this regard, Fig. 5 suggests that each if all channels have the same launch power (according to mutual power optimization), rather than individually optimized powers, then minimum penalties are observed. Also, the mutually optimized launch power is actually very close to the homogenous optimal launch power of 1dBm, since individual modes had similar

optimum power corresponding to similar effective areas (found in Fig. 3 for mode coupling strength of 5%, and data for other mode coupling strengths, not shown here for the sake of conciseness).

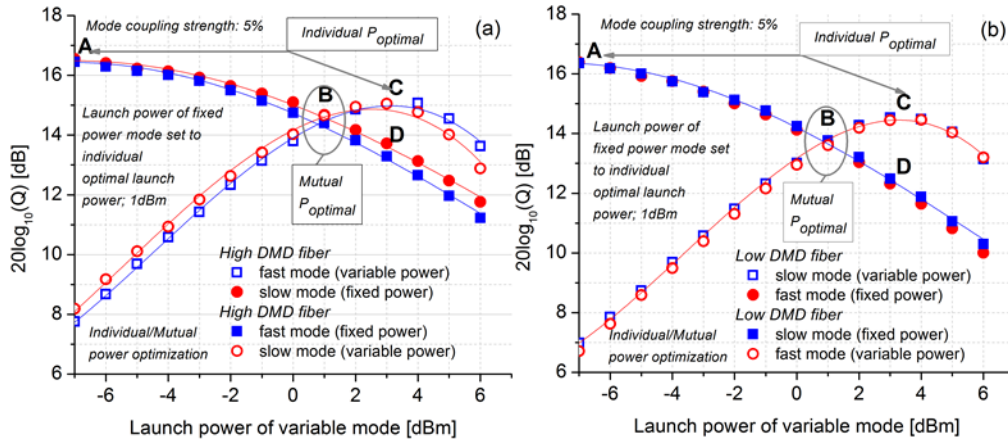


Fig. 5. Q-factor [dB] as a function of launch power [dBm], for QPSK transmission over 1,600km, employing a) High DGD fiber (square: fast mode, circle: slow mode) and b) Low DMD fiber (square: slow mode, circle: fast mode), where solid symbols represent the channel with fixed power (1dBm) and open symbols the channel with variable power. (This figure represents a case of individual/mutual power optimization)

In Fig. 6 we plot various delta Q-factors as a function of mode coupling strength. Due to the similarity in performance of both channels, we consider only variable signal power in fast mode (high DMD fiber) and slow mode (low DMD fiber), respectively, and plot the performance penalties with reference to the individual optimal powers of both fixed and variable power modes (best performance). Note that in order to get each data point on Fig. 6, simulations similar to Fig. 3 and Fig. 5 were carried out for each mode coupling strength, for both low and high DMD fibers. In Fig. 6(a), Q-penalties are plotted for the high DMD fiber, where penalties represent: 1) Q1\_HighDMD, representing performance penalty for fixed power mode (or slow mode) in case of individual launch power optimization for variable power mode (or fast mode). It is calculated by subtracting Q-factor (slow mode) at individual  $P_{\text{optimal}}$  of slow mode and Q-factor (slow mode) at individual  $P_{\text{optimal}}$  of fast mode, 2) Q2\_HighDMD, representing performance penalty for fixed power mode (or slow mode) in case of mutual launch power optimization for fixed power mode and variable power mode (or fast mode). It is calculated by subtracting Q-factor (slow mode) at individual  $P_{\text{optimal}}$  of slow mode and Q-factor (slow mode) at mutual  $P_{\text{optimal}}$  of slow and fast modes, 3) Q3\_HighDMD, representing performance penalty for variable power mode (or fast mode) in case of mutual launch power optimization for fixed power mode (or slow mode) and variable power mode. It is calculated by subtracting Q-factor (fast mode) at individual  $P_{\text{optimal}}$  of fast mode and Q-factor (fast mode) at mutual  $P_{\text{optimal}}$  of fast and slow modes. Similar approach is taken in Fig. 6(b) for low DMD fiber (corresponding penalties are Q1\_LowDMD, Q2\_LowDMD and Q3\_LowDMD). As shown in Fig. 5, the penalties reported are predominantly influenced by intra mode nonlinearity and linear crosstalk, however, intra mode nonlinear effects have a non-negligible impact (Fig. 4(b)). It can be observed that, as the mode coupling strength is increased, the Q-penalties monotonically increase, in particular for the fixed power mode, irrespective of the DMD (Fig. 6(a) and Fig. 6(b)) or approach to power control. Interestingly, the performance of the variable power mode is not degraded significantly, with penalties below 1.5dB for any given scenario. At this transmission reach, the performance of a fixed power channel is severely degraded for coupling strength beyond few percentiles. This behavior can be attributed to increasing inter mode coupling with mode coupling strength, owing to the increasing power of the variable power mode. Figure 6(a) shows that at 10% mode coupling efficiency Q-penalties of ~5.5 dB (Q1\_HighDMD), ~3.5 dB (Q2\_HighDMD),



and ~1.5 dB (Q3\_HighDMD) are observed. These results clearly show that even though the impact of launch power allocation strategy is not extreme for low mode coupling values (<~2dB up to mode coupling strength of 2.5%), it significantly degrades the transmission performance with increasing mode coupling strength. with the mutual power optimization strategy offering lower overall penalties.

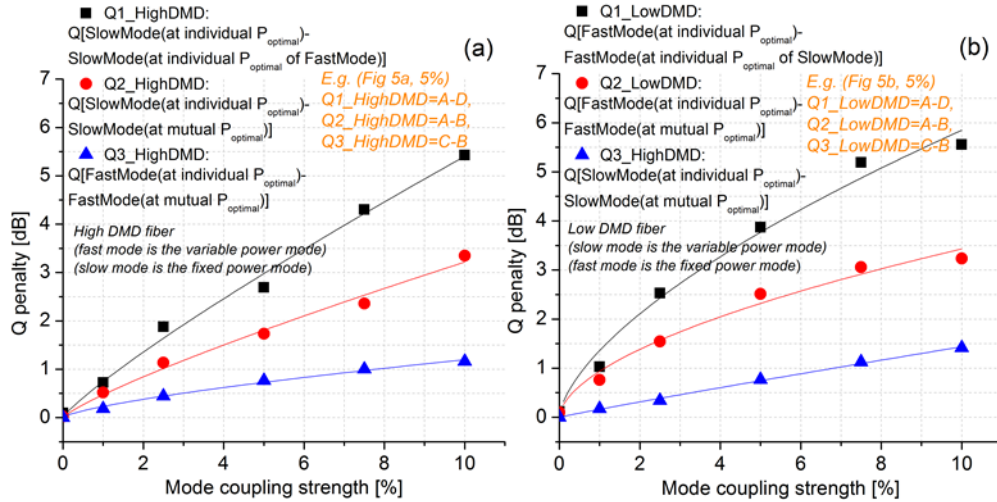


Fig. 6. Q-factor penalty [dB] as a function of mode coupling strength [%], for QPSK transmission over 1,600km. a) High DMD fiber (fast mode is with variable power). Squares:  $Q1_{HighDMD} = Q [SlowMode(at\ individual\ P_{optimal}) - SlowMode(at\ individual\ P_{optimal}\ of\ FastMode)]$ , Circles:  $Q2_{HighDMD} = Q [SlowMode(at\ individual\ P_{optimal}) - SlowMode(at\ mutual\ P_{optimal})]$ , Up-triangle:  $Q3_{HighDMD} = Q [FastMode(at\ individual\ P_{optimal}) - FastMode(at\ mutual\ P_{optimal})]$ . b) Low DMD fiber (slow mode is with variable power). Squares:  $Q1_{LowDMD} = Q [FastMode(at\ individual\ P_{optimal}) - FastMode(at\ individual\ P_{optimal}\ of\ SlowMode)]$ , Circles:  $Q2_{LowDMD} = Q [FastMode(at\ individual\ P_{optimal}) - FastMode(at\ mutual\ P_{optimal})]$ , Up-triangle:  $Q3_{LowDMD} = Q [SlowMode(at\ individual\ P_{optimal}) - SlowMode(at\ mutual\ P_{optimal})]$ .

#### 4. Conclusions

We have reported on the dynamics of power allocation strategies in few-mode fiber based long-haul transmission systems. It is shown that in the absence of linear coupling, the transmission performance is independent of power allocation approach, however in the weakly coupled regime, individual power allocation approach may induce penalties up to ~2dB. In contrast, when mode coupling strength is increased, transmission performance is significantly degraded, if modes are allowed to individually optimize their corresponding launch powers, with penalties up to ~5.5dB. Whilst optimum power differences of up to 0.5 dB may have been expected due to differences in effective area, we found no evidence favoring individual power optimization and that homogenous (or mutual in this case) power allocation should be used.

#### Acknowledgments

This work was partially supported by EU FP7-ICT project, MODE-GAP.